



CONSTRAINED OPTIMAL CONTROL OF VIBRATION DAMPERS

P. KASTURI AND P. DUPONT

*Aerospace and Mechanical Engineering, 110 Cummington Street, Boston, MA 02215,
U.S.A.*

(Received 22 July 1997, and in final form 20 March 1998)

Optimal control of dampers has been proposed to mitigate vibration effects in mechanical systems. In many cases, systems are subject to periodic forcing and the goal is to maximize the energy dissipated by the damper. In contrast to prior work utilizing instantaneous or infinite-time – horizon optimization, this paper employs periodic optimal control to maximize the energy dissipated per cycle. For single-degree-of-freedom systems in which the maximum allowable control effort is of the same order as the forcing magnitude, a state-dependent singular control law is shown to deliver maximum energy dissipation. Alternate control laws are proposed for situations when rattle space requirements dictate damper displacements other than that of the singular solution. Saturation of the damping force is also considered.

© 1998 Academic Press

1. INTRODUCTION

Dampers are used in a wide variety of applications to isolate structures and equipment from vibrations and to dissipate energy. Applications include flutter mitigation in turbine blades of aircraft engines and power plant generators [1, 2], vibration damping in large space structures [3] and helicopters [4], and shock and vibration isolation for vehicles and equipment cradles [5–7].

Dampers can be designed to be either passive (e.g., dashpots), active (e.g., motors) or semi-active (e.g., hydraulic cylinders with controllable orifice diameter). Semi-active dampers are the most appealing to designers because they deliver performance that rivals active dampers, while consuming only a fraction of the power required by them [7].

In this paper, periodic optimal control is employed to maximize the energy dissipated by a damper. In order to establish a benchmark for controller performance, no constraints are imposed on the damping force. For implementation, controller saturation as well as any relevant damper dynamics would have to be considered.

In the next section, control approaches which have been applied to dampers are reviewed. The following section presents the derivation of the singular controller which maximizes energy dissipation according to the system parameters and the periodic forcing. A penalty on control effort is then introduced to obtain controllers for a range of damper displacement amplitudes (rattle space). Next, the case of control saturation is discussed. Numerical results are presented for each case followed by conclusions.

2. CONTROL OF DAMPERS

Several control approaches have been pursued to maximize damper energy dissipation. These include Lyapunov's direct method, sliding mode control and LQR theory. The first method entails optimizing energy dissipation in an instantaneous sense by choosing the control which maximizes the derivative of a Lyapunov energy function. Semi-active controllers of this type have been developed for use with electrorheological (ER) fluid dampers [8] as well as friction dampers [9]. Sliding mode control, on the other hand, was successfully employed by Wang and co-workers [10] to improve the performance of ER dampers.

Another control approach that has received considerable attention is LQR theory. Ferri and co-workers have applied this technique to friction dampers [5]. The cost function used was an infinite time integral of a weighted sum of system energy and control effort. Numerical simulations indicated a marked improvement in energy dissipation over a simple feedback controller given by $F_N(t) = k|\dot{x}|$, where \dot{x} is the relative velocity and $F_N(t)$ is the normal force at a friction interface. In the vibration isolation of automobiles, Hrovat proposed LQR controllers using cost functions composed of mean-square rattle space and a metric of ride discomfort [6]. Similarly, Karnopp and Trikha have proposed the use of LQR theory in enhancing shock and vibration isolation in an aircraft landing/taxiing on a runway [7].

In many situations, the vibrational energy is concentrated at a few frequencies corresponding either to the natural frequencies of the structure or to the forcing frequencies. For example, in helicopters the critical forcing frequencies are $\bar{\omega}$ and $n\bar{\omega}$. Here $\bar{\omega}$ is the rotational frequency of the rotor and n is the number of blades. In this context, Johnson has surveyed modelling and active damping techniques designed to minimize structural vibration and loads [4]. For a given helicopter flight condition, a linear quasistatic model which relates rotor blade pitch angles to vibration and load is estimated in the frequency domain. The control approach employs a cost function quadratic in the harmonics of the inputs and outputs. The cost function is minimized using either current and prior values of the inputs and outputs. As a consequence, it is a type of instantaneous optimization. The resulting control signal is superimposed on the nominal rotor blade oscillation necessary for trim.

In applications such as this, the controlled steady state response will be periodic and the control law should take advantage of this fact. Instantaneous optimization approaches do not take the periodicity into account and so the results tend to be suboptimal. Similarly, those who have applied LQR theory have considered only transient response or stochastic excitation. In contrast, the periodic controllers developed here maximize steady state dissipation according to the particular forcing.

3. PERIODIC OPTIMAL CONTROL

In this section, a standard variational approach is employed to derive the optimal damping force for systems with periodic excitation. Given the forcing, it is expected that the system trajectory will be periodic. It is interesting to note, however, that the classical applications of periodic optimal control are systems which possess closed-loop equilibrium points. For example, Horn and Lin showed that in chemical reactor operation, periodic control laws improve performance in comparison to steady state optimal controllers [11]. Similar strategies were employed in the analysis of fuel-efficient cruise trajectories for aircraft, wherein the standard optimal controllers (LQR, etc.) were replaced by periodic controls [12].

3.1. CONTROLLER DESIGN

Consider maximizing the energy dissipated by a control force, u on the system shown in Figure 1. A state variable representation of this system is given by

$$\dot{x}_1 = x_2, \quad \dot{x}_2 = \frac{1}{m} (F_{ext}(t) - cx_2 - kx_1 - u), \tag{1, 2}$$

where $F_{ext}(t)$ is a known external periodic force.

Since this is a non-autonomous system, these equations can be redefined as

$$\dot{x}_1 = x_2, \quad \dot{x}_2 = \frac{1}{m} (F_{ext}(x_3) - cx_2 - kx_1 - u), \quad \dot{x}_3 = 1, \tag{3-5}$$

where $x_3 = t$.

To maximize the energy dissipated, the negative integral of damping power is minimized over the system period. Together with a quadratic penalty on control force, the cost function is given by

$$J(u) = \min_{u \in \Omega} \frac{1}{\tau} \int_{t_0}^{t_0 + \tau} \left[-ux_2 + \frac{\varepsilon}{2} u^2 \right] dt, \tag{6}$$

where $\tau \in T \triangleq (0, \infty)$ is the time period of the system and t_0 is the initial time. Ω is the set of all admissible values for u , in which the maximum value of u is of the same order as the forcing magnitude and $u(t)$ is piecewise continuous.

An optimal controller with no constraints on the control effort expended ($\varepsilon = 0$) will first be developed. It is assumed that the state variables as well as the time period are free variables. Furthermore, periodicity of the state variables, x_1 and x_2 , is treated as an input to the problem. Penalty on control effort ($\varepsilon \neq 0$) will be introduced in the subsequent sections.

With $\varepsilon = 0$, the Hamiltonian can be written as

$$H(x, \lambda, u, x_3, \lambda_3) = -ux_2 + \lambda_1 x_2 + \frac{\lambda_2}{m} (F_{ext}(x_3) - cx_2 - kx_1 - u) + \lambda_3. \tag{7}$$

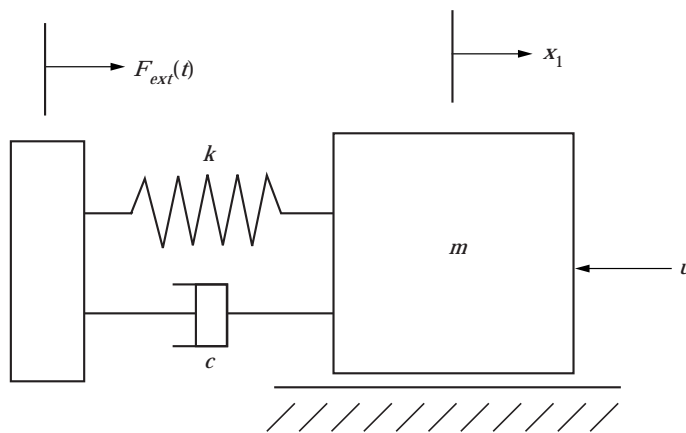


Figure 1. Block model for studying forced vibrations.

Necessary conditions for optimality indicate that

$$\dot{\lambda}_1 = \frac{k}{m} \lambda_2, \quad \dot{\lambda}_2 = -\lambda_1 + \frac{c}{m} \lambda_2 + u, \quad \dot{\lambda}_3 = -\frac{1}{m} \frac{\partial F_{ext}(x_3)}{\partial x_3} \lambda_2, \quad (8-10)$$

$$x_2 + \frac{\dot{\lambda}_2}{m} = 0, \quad x_1(t_0) = x_1(t_0 + \tau), \quad x_2(t_0) = x_2(t_0 + \tau), \quad (11-13)$$

$$\lambda_1(t_0) = \lambda_1(t_0 + \tau), \quad \lambda_2(t_0) = \lambda_2(t_0 + \tau), \quad H(x, \lambda, u, x_3, \lambda_3) = K, \quad H(t_0 + \tau) = J(u), \quad (14-17)$$

along the optimal trajectory [13]. Here, K is a constant to be determined.

Since the Hamiltonian is linear in u , $H_u = 0$ does not yield an expression for the optimal controller. Instead, it defines a singular arc, given by equation (11). This equation implies that

$$\dot{x}_2 + \frac{\dot{\lambda}_2}{m} = 0. \quad (18)$$

From equations (8)–(11) and (18), the expression for u can be determined to be*

$$u = F_{ext}(x_3) - cx_2 - kx_1 - \frac{m}{2c} \frac{\partial F_{ext}(x_3)}{\partial x_3}. \quad (19)$$

With $x_3(t) = t$, and u as defined above, the system dynamics, equations (3)–(5), can be solved to give

$$x_1(t) = x_1(t_0) + \left[-\frac{1}{2c} F_{ext}(t_0) + x_2(t_0) \right] t + \frac{1}{2c} \int_{t_0}^t F_{ext}(\sigma) d\sigma, \quad (20)$$

$$x_2(t) = x_2(t_0) + \frac{1}{2c} [F_{ext}(t) - F_{ext}(t_0)]. \quad (21)$$

Note that equations (19)–(21) hold for any periodic input. Since any such input can be written as a Fourier series, let $F_{ext}(t) = A \sin(\bar{\omega}t + \phi)$, without any loss of generality. The optimal period of the system for this case is the same as the forcing period.

The initial conditions, $x_1(t_0)$ and $x_2(t_0)$, in the above equations can now be chosen such that the periodicity conditions, (12) and (13), are satisfied. With $F_{ext}(t)$ as defined above and $\phi = 0$, these initial values can be shown to be

$$x_1(t_0) = -\frac{A}{2c\bar{\omega}} \cos(\bar{\omega}t_0), \quad x_2(t_0) = \frac{A}{2c} \sin(\bar{\omega}t_0), \quad (22, 23)$$

Since x_1 , x_2 , and u are known along the singular arc, the transversality conditions of equations (16) and (17) give the average rate of energy dissipation,

$$J(u) = K = \frac{A^2}{8c}, \quad (24)$$

for $\bar{\omega} = 2\pi/\tau$ and $t_0 = 0$.

* Since this control law is valid only along the singular arc, it will be referred to as the ‘‘singular controller’’ from here onward in this paper.

Finally, since the Hamiltonian (7), is linear in u , the generalized Legendre–Clebsch condition, $(\dot{H}_u)_u \leq 0$, can be employed as a weak local sufficiency condition. This is satisfied along the singular arc,

$$\frac{\partial}{\partial u} \frac{d^2 H_u}{dt^2} = -\frac{2c}{m^2} < 0. \quad (25)$$

3.1.1. Numerical evaluation of singular control

To facilitate the comparison of controller performance due to variations in parameter values, let the ratio between the forcing frequency and the undamped natural frequency of the system be given by $\beta = \bar{\omega}/\omega_n$, where $\omega_n = \sqrt{k/m}$. Also, let the damping ratio of the system be given by $\zeta = c/(2m\omega_n)$. The state trajectories, optimal control force, net energy dissipated by the controller, and control effort spent can now be rewritten in terms of these quantities as

$$x_1(t) = -\frac{A}{4\zeta\beta m\omega_n^2} \cos(\bar{\omega}t), \quad x_2(t) = \frac{A}{4\zeta\omega_n m} \sin(\bar{\omega}t), \quad (26, 27)$$

$$u(t) = \frac{A}{2} \sin(\bar{\omega}t) + (1 - \beta^2) \frac{A}{4\zeta\beta} \cos(\bar{\omega}t), \quad (28)$$

$$E = \int_0^\tau u x_2 dt = \frac{A^2}{16\zeta\omega_n m} \tau = K\tau, \quad (29)$$

$$U = \int_0^\tau u^2(\sigma) d\sigma = \frac{A^2}{8} \left[1 + \frac{(1 - \beta^2)^2}{4\zeta^2\beta^2} \right] \tau, \quad (30)$$

where E is the energy dissipated per cycle and U is the control effort expended per cycle. Note that for general periodic forcing,

$$F_{ext}(t) = \sum_{p=1}^{\infty} A_p \sin(\bar{\omega}_p t), \quad (31)$$

the optimal control force can be shown to be

$$u(t) = \sum_{p=1}^{\infty} \left[\frac{A_p}{2} \sin(\bar{\omega}_p t) + (1 - \beta^2) \frac{A_p}{4\zeta\beta} \cos(\bar{\omega}_p t) \right]. \quad (32)$$

The following results were obtained with parameters chosen as follows: $A = 105$, $m = 1$, $c = 0.1$, $\bar{\omega} = 2\pi$. k was chosen to give a desired value of β .

Figure 2 depicts control force versus displacement along the singular arc, for $\beta = 0.8$, 1.0 , and 1.25 , while holding ζ constant ($= 0.00796$). The area inside this curve represents the amount of energy dissipated per cycle by the controller—equal to E . It can be shown that the optimal control force corresponds to a passive system*. From equations (27) and (28), the optimal control impedance is

$$c^* = \frac{u(t)}{x_2(t)} = 2\zeta\omega_n m + (1 - \beta^2) \frac{\omega_n m}{\beta} \cot(\bar{\omega}t) = c + (1 - \beta^2) \frac{\omega_n m}{\beta} \cot(\bar{\omega}t). \quad (33)$$

* A system is said to be passive if, for all time, the power entering the system is greater than or equal to the rate of change of energy stored in the system.

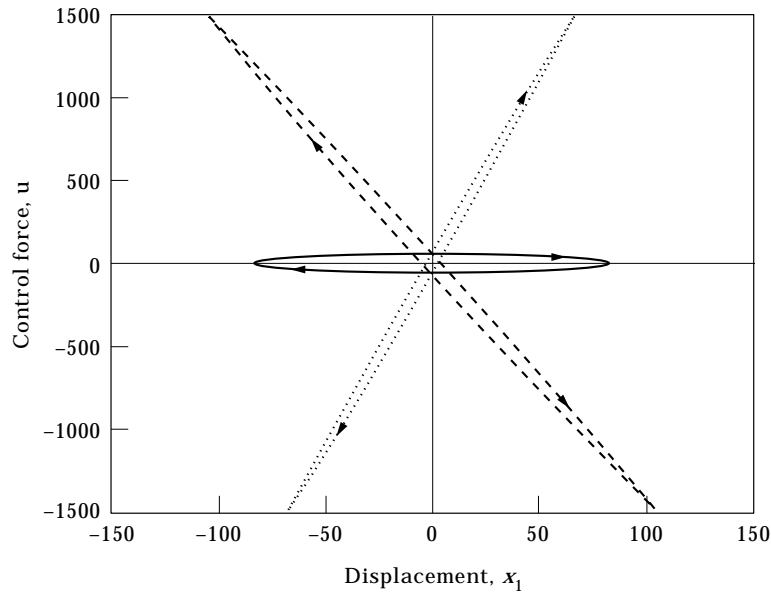


Figure 2. Control force versus displacement for $\beta = 0.8$ (---), 1, (—), 1.25 (...) along singular arc trajectory; ζ is held constant at 0.00796.

From this equation it can be observed that the optimal control force is viscous in nature for $\beta = 1$. Otherwise, the corresponding passive system would store and release energy during each period. For example, a passive implementation of c^* could be comprised of a spring ($\beta > 1$) or mass ($\beta < 1$) in parallel with a viscous damper.

While not apparent from this figure, equation (29) indicates that the amount of energy dissipated per cycle, E , depends on τ . Therefore, as β increases ($\bar{\omega}$ is increased holding ω_n

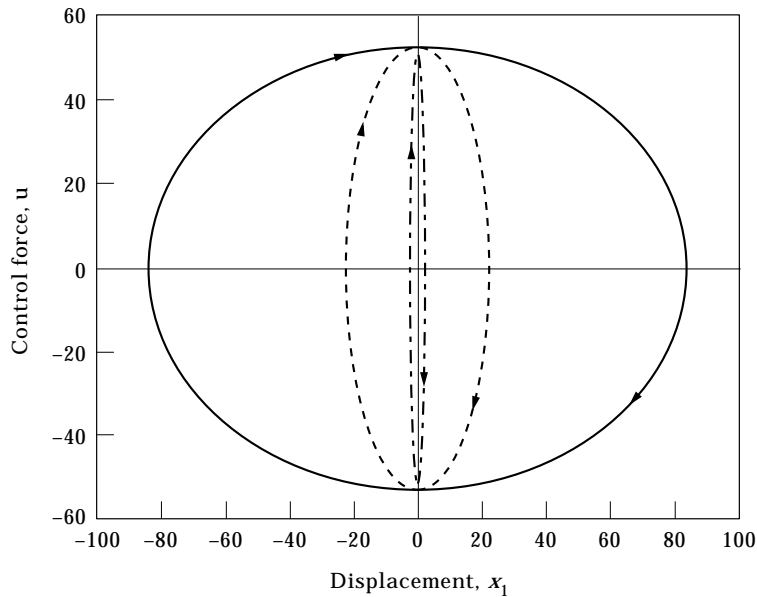


Figure 3. Control force versus displacement for $\zeta = 0.00796$ (—), 0.03, (---), 0.3 (-·-·-) along singular arc trajectory; β is held constant at 1.

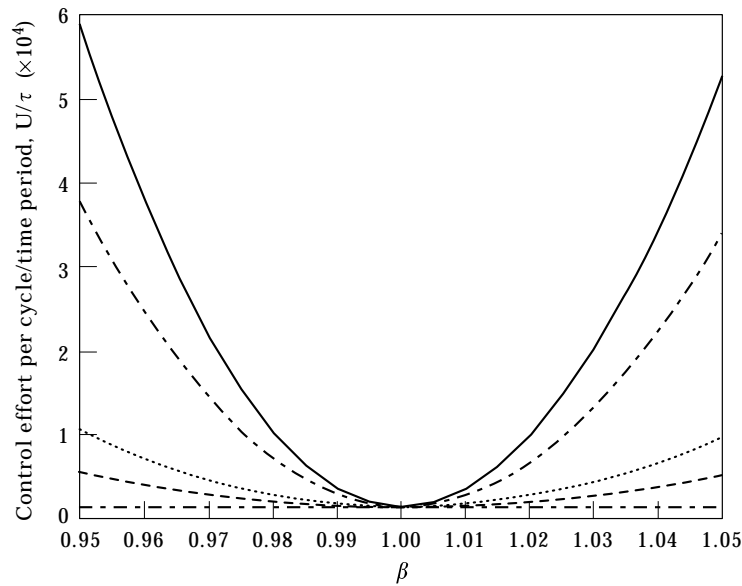


Figure 4. Average control effort expended versus β for different values of ζ : —, 0.00796; --, 0.01; ····, 0.02; ---, 0.03; -·-·-, 0.30.

constant), the amount of energy dissipated per cycle decreases. Thus, for the areas in Figure 2, $A_1 < A_2 < A_3$ corresponding to $\beta = 1.25, 1.0$ and 0.8 , respectively. The average rate of energy dissipation, E/τ , however, remains constant. It can also be observed from this figure and equation (26) that the peak-to-peak amplitude of oscillation decreases with increase in the value of β .

Figure 3 represents optimal control force versus displacement for $\zeta = 0.00796, 0.03$ and 0.3 , with β and ω_n held constant. It is clear from this figure, as well as from equations (26) and (29), that the peak-to-peak amplitude of oscillation besides the average rate of energy dissipation, E/τ , decrease with increasing ζ . In other words, as the amount of internal damping in a system increases, the scope for improvement in energy dissipation through an external damping force decreases.

The ratio between amount of control effort expended per cycle and time period of the system, U/τ , for different values of β and ζ is presented in Figure 4. This figure indicates that the minimum control effort is expended when $\beta = 1$, independent of the value of ζ . For $\beta \neq 1$, however, the control effort decreases with increasing ζ .

Since E/τ remains the same for any value of β , and it increases as ζ decreases, a key factor in determining operating conditions under which the singular optimal controller will be most effective is U/τ . It can, therefore, be deduced from Figure 4 that an external damper will be most effective when $\beta = 1$ and ζ is very small. Of course most systems for which energy dissipation is of import have very low internal damping (directly related to ζ) and operate near resonance ($\beta = 1$).

3.1.2. Rattle space constraints

In many practical systems, the rattle space* may be smaller than what is commanded by the singular controller described above. To determine an optimal control force for systems with rattle space constraints, the problem is redefined as follows: for a given value of $x_1(t_0)$ and $x_2(t_0)$, determine the maximum amount of energy that can be dissipated by an external control force, while ensuring periodicity about $x_1(t_0)$ and $x_2(t_0)$. Since the choice

* Rattle space is defined as the permissible peak-to-peak displacement of a system.

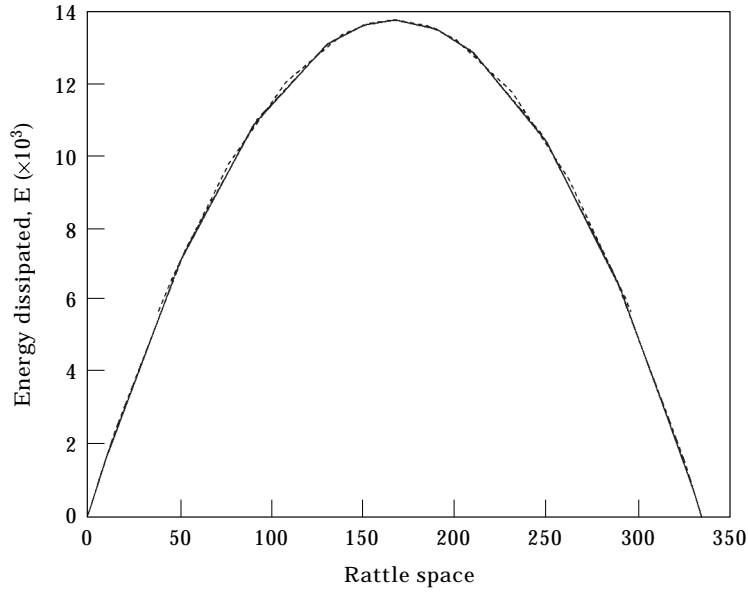


Figure 5. Energy dissipated per cycle versus rattle space (x_1 peak-to-peak) for $\epsilon = 0.01$ (\cdots), 0.1 ($- \cdot -$), 1 ($- - -$), 100 (---).

of initial values for x_i obviates the necessary condition on periodicity of λ_i , a numerical solution entails solving for λ_i such that x_1 and x_2 are periodic.

To solve this problem, a penalty on control effort is introduced ($\epsilon \neq 0$ in equation (6)). The optimal control force for this case can be determined to be

$$u_\epsilon = \left(x_2 + \frac{\lambda_2}{m} \right) / \epsilon. \tag{34}$$

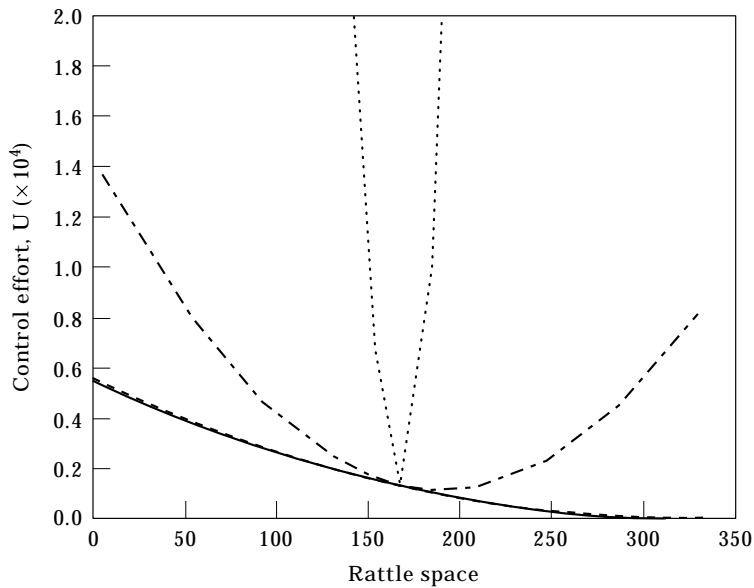


Figure 6. Control effort expended versus rattle space (x_1 peak-to-peak) for $\epsilon = 0.01$ (\cdots), 0.1 ($- \cdot -$), 1 ($- - -$), 100 (---).

Numerical analysis was used to compare the performance of the constrained rattle space controller with that of the singular controller. Four different values of ε were considered (0.01, 0.1, 1 and 100).

Figure 5 depicts energy dissipated versus rattle space, for $\beta = 1$, $\zeta = 0.00796$ and the four values of ε . It is evident from this figure that there exists a unique value of displacement amplitude (≈ 167) where the maximum energy is dissipated. This amplitude is equal to that of the singular arc amplitude (refer to the peak-to-peak value of x_1 for $\beta = 1$ in Figure 2). In fact, at this amplitude, the trajectories are those of the singular arc, independent of ε .

It is also clear from this figure that the amount of energy dissipated by the constrained rattle space controller is practically independent of the value of ε . Figure 6, however, indicates that control effort expended for $\beta = 1$ and $\zeta = 0.00796$ is highly dependent on ε at rattle space amplitudes other than that of the singular arc. From Figures 5 and 6, it is clear that the control trajectory obtained for large ε should be used in any implementation.

Numerical results for large ε and $\beta = 1$ indicate that the optimal displacement trajectory is sinusoidal and that the optimal damping force is viscous. Given these two observations, the optimal viscous damping force can be shown analytically to be

$$c^* = \frac{2A}{\bar{\omega}x_{pp}} - c, \quad (35)$$

where A and $\bar{\omega}$ are the amplitude and frequency of the external forcing, F_{ext} , and the desired rattle space is x_{pp} . In contrast to equation (34), this expression can be directly implemented as a feedback control law for systems with $\beta = 1$.

It is also clear from this equation that, for positive energy dissipation, the specified rattle space must satisfy

$$x_{pp} < \frac{2A}{\bar{\omega}c}. \quad (36)$$

3.1.3. Controller saturation

The magnitude of the optimal damping force described by equation (34) is bounded. In implementation, however, it is still possible that the maximum output of the prescribed damper is less than this magnitude. It is therefore of interest to know how the optimal control is modified by saturation limits. Furthermore, bang-bang controllers have been proposed in several previous studies [8–10]. Thus, it is also of interest to know when the saturated optimal control is of the bang-bang variety.

In this case, equation (34) is modified according to Pontryagin's Maximum Principle as follows:

$$u_{sat} = \begin{cases} M, & \text{if } (x_2 + \lambda_2/m)/\varepsilon \geq M, \\ (x_2 + \lambda_2/m)/\varepsilon, & \text{if } -M < (x_2 + \lambda_2/m)/\varepsilon < M, \\ -M, & \text{otherwise,} \end{cases} \quad (37)$$

where M is the maximum allowed control force.

Consider the case when M is slightly smaller than $u_{max}(x_{pp})$, the magnitude called for by equation (34) for a fixed value of rattle space, x_{pp} . Simulation shows that except for two segments per cycle, $x_2 + \lambda_2/m = O(\varepsilon)$. Thus, the trajectory of u_{sat} remains unsaturated except during these two segments. If M is decreased, the duration of the unsaturated portion decreases and the duration of the saturated portion increases.

The same effect is achieved by holding M constant and decreasing the rattle space. The minimum rattle space solution corresponds to a bang-bang solution, i.e., $u_{sat} = M \operatorname{sgn}(x_2)$. Note that if $M \ll u_{max}(x_{sa})$, where x_{sa} is the singular arc rattle space, the minimum rattle space can be greater than the singular arc rattle space.

As expected, holding the rattle space fixed, more control effort, defined by $U = \int_0^{\epsilon} u^2(\sigma) d\sigma$, is expended by a saturating controller than for a non-saturating controller obtained for $\epsilon \geq 1$. In other words, while the non-saturating controller produces a larger peak force, it requires less control effort per cycle.

4. CONCLUSIONS

In this paper, periodic optimal controllers were designed to maximize energy dissipated by a damper. For single-degree-of-freedom systems, a singular control law was shown to deliver the maximum energy dissipation. The singular controller can be implemented as a passive system. Except when forced at resonance, however, the damping system would include energy storage elements.

Constrained optimal controllers were proposed for systems with rattle space less than what is commanded by the singular controller and for dampers with saturation limits. The controller performance indicates that the energy dissipated is virtually independent of any penalty imposed on the control effort. The control trajectories obtained for the largest penalty can, therefore, be used to deliver maximum energy dissipation for the allowed rattle space and saturation limits, while expending the least control effort.

The periodic forcing acting on the system was assumed to be composed of one frequency. Since any periodic input can be written as a Fourier series, the results obtained in this paper can be appropriately extended to such inputs. Future work involves finding representations of the constrained optimal control laws which can be written explicitly in terms of the state variables, desired rattle space and saturation limit.

ACKNOWLEDGMENT

This work was supported in part by the Dynamic Systems and Control Program of the National Science Foundation under grant MSS-9302190.

The authors wish to thank Professor David Castañón for his valuable suggestions at various stages of this project.

REFERENCES

1. A. SINHA and J. GRIFFIN 1982 *Journal of Aircraft* **20**, 372–376. Friction damping of flutter in gas turbine engine airfoils.
2. A. SRINIVASAN and D. CUTTS 1984 *Journal of Vibration, Acoustics, Stress, and Reliability in Design* **106**, 189–197. Measurement of relative vibratory motion at the shroud interfaces of a fan.
3. A. FERRI 1987 *Proceedings, 11th Biennial Conference on Mechanical Vibration and Noise, Boston, MA DE-VOL. 5*, 187–195. Investigation of damping from nonlinear sleeve joints of large space structures.
4. W. JOHNSON 1982 *NASA Technical Report NASA-TP-1996*. Self-tuning regulators for multicyclic control of helicopter vibration.
5. J. LANE, A. FERRI and B. HECK 1992 *Proceedings, ASME Winter Annual Meeting, Anaheim, DE-Vol. 49*, 165–171. New York: ASME, Vibration control using semi-active frictional damping.
6. D. HROVAT 1993 *Journal of Dynamic Systems, Measurement, and Control* **115**, 328–342. Applications of optimal control to advanced automotive suspension design.
7. D. KARNOPP and A. TRIKHA 1969 *Journal of Engineering for Industry* **91B**, 1128–1132. Comparative study of optimization techniques for shock and vibration isolation.

8. N. McCLAMROCH, H. GAVIN, D. ORTIZ and R. HANSON 1994 *Proceedings, 33rd Conference on Decision and Control, Lake Buena Vista, FL*, 97–102. Electrorheological dampers and semi-active structural control.
9. P. DUPONT, P. KASTURI and A. STOKES 1997 *Journal of Sound and Vibration* **202**, 203–218. Semi-active control of friction dampers.
10. K. WANG, Y. KIM and B. SHEA 1994 *Journal of Sound and Vibration* **177**, 227–237. Structural vibration control via electrorheological-fluid-based actuators with adaptive viscous and frictional damping.
11. F. HORN and R. LIN 1967 *Industrial and Engineering Chemistry Process Design Development* **6**, 21–30. Periodic processes: a variational approach.
12. J. SPEYER and R. EVANS 1984 *IEEE Transactions on Automatic Control* **AC-29**, 138–148. A second variational theory for optimal periodic processes.
13. M. ATHANS and P. FALB 1966 *Optimal Control: An Introduction to the Theory and its Applications*. New York: McGraw-Hill Book Company.